

Maciej KLIMAS, Dariusz GRABOWSKI, Anna PIASKOWY  
Silesian University of Technology

## EFFICIENCY ANALYSIS OF AN ELECTROMAGNETIC LAUNCHER

**Summary:** A multistage electromagnetic launcher (EML) construction followed by its model analysis have been presented in the paper. The EML under consideration belongs to the class of so called coilguns – the force used to accelerate a projectile is obtained with the help of coils. The EML simulations have been made by means of FEMM and Scilab software. Consequently, waveforms of mechanical quantities describing the projectile movement, such as displacement, instantaneous velocity and acceleration, as well as electrical quantities describing phenomena in successive coil circuits have been obtained. The results are consistent with theoretical considerations as well as results reported by other authors. The future work will include comparison of simulation and measurement results followed by evaluation of simplifying assumptions undertaken in the paper.

**Keywords:** electromagnetic launcher, coilgun, EML, FEM analysis, Scilab

## ANALIZA SPRAWNOŚCI WYZUTNI ELEKTROMAGNETYCZNEJ

**Streszczenie:** W artykule przedstawiono budowę wielostopniowej wyrzutni elektromagnetycznej oraz analizę jej modelu. Wyrzutnia należy do klasy tak zwanych działa elektromagnetycznych, w których siła napędzająca pocisk uzyskiwana jest z wykorzystaniem cewek (działo Gaussa). W efekcie symulacji przeprowadzonych w środowisku FEMM oraz Scilab uzyskano przebiegi wielkości mechanicznych (przemieszczenia, chwilowej prędkości i przyśpieszenia) opisujących ruch pocisku oraz prądów w obwodach cewek w kolejnych stopniach wyrzutni. Otrzymane wyniki są zgodne z wynikami analizy teoretycznej oraz wynikami uzyskanymi przez innych autorów. W przyszłości planowane jest porównanie uzyskanych wyników symulacyjnych z przebiegami pomiarowymi, a następnie przeprowadzenie na tej podstawie oceny założeń upraszczających w analizowanym modelu wyrzutni.

**Slowa kluczowe:** wyrzutnia elektromagnetyczna, działo Gaussa, analiza FEM, Scilab

### 1. INTRODUCTION

Weapons, in which a projectile is accelerated in a way other than through expansion of gasses produced by explosive materials, enjoy remaining interest among scientific researchers

and military forces around the world [2]. Electromagnetic launchers (EML) are examples of devices with that kind of acceleration method [7]. They can be divided into two categories: railguns and coilguns [10]. The railgun is a type of rifle in which acceleration of a projectile is caused by the Lorentz force, while the coilgun, or in other words the Gauss rifle, operates by means of the reluctance force. There are also launchers making use of both methods of acceleration or even having an additional pneumatic module which allows to set the projectile initial velocity [1], [9], [11].

Although the history of the EMLs goes back to the beginning of the previous century, there is still lots of open problems regarding the EMLs and thus many scientific papers on this topic are published every year. These problems concern first of all optimization of the EML geometry and power parameters [2], [8], [16], [19]. There is also a constant search for new applications of the EMLs [2], [6], [7].

In the case of coilguns, investigations are focused, among others, on the efficiency of guns with different numbers of coils (stages). It has been proved that the 3-stage coilgun is more energy efficient than the single-stage one. For the same amount of energy expended the three-stage coilgun achieves a higher muzzle velocity [16]. Experimental results for a 4-stage coilgun have been presented in [20], while the design and testing of a 15-stage one can be found in [18]. The energy efficiency of the 4-stage coilgun, defined as a ratio of the projectile kinetic energy to the capacitor stored energy, has been estimated to be 5% and 6% [20]. Increasing the number of coils to 15 allows to reach the energy efficiency of almost 15% [18] and for 466 coils the reported efficiency is 31%, but with energy recovery it could be increased to 74% [8]. It must be stressed that the comparison of efficiencies of different coilguns is not an easy task as the efficiency depends not only on the number of stages but also on the projectile size and material.

This article belongs to the above mentioned trend – it presents the construction of a 5-stage coilgun and its computer model along with some simulation results with special emphasis on key factors from the efficiency point of view. Moreover, a new approach to coilgun simulation based on the application of FEMM and Scilab software has been proposed. The article is a complement to a previous paper [4].

The future work will include comparison of simulation and measurement results for all five stages followed by evaluation of simplifying assumptions undertaken in the paper. The time-varying model including the effect of the projectile movement on the equivalent inductance of each coil will be also considered.

## 2. ELECTROMAGNETIC LAUNCHER DESCRIPTION

The electromagnetic launcher under consideration (Fig. 1) consists of a few basic functional modules: the main RLC circuit, the measurement and control circuits as well as the power supply with capacitor charging unit. These modules have been briefly described in the next section.

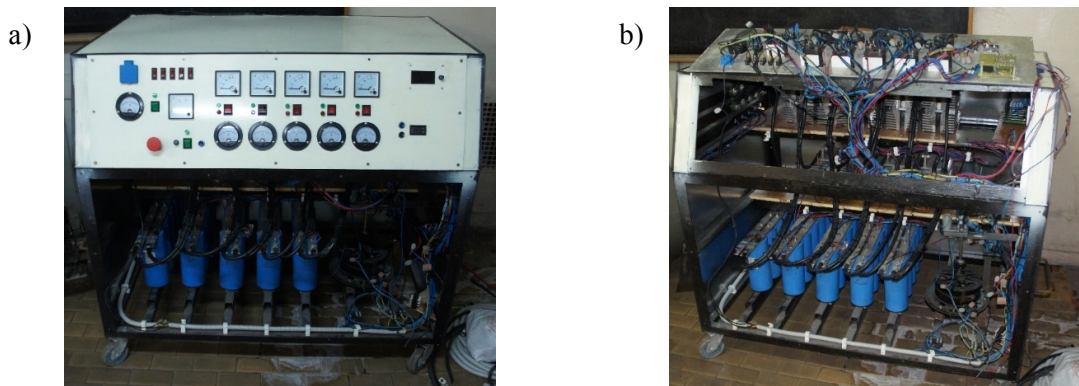


Fig. 1. Electromagnetic launcher – general view with the control panel (a) and inside view (b)  
Rys. 1. Wyrzutnia elektromagnetyczna – widok ogólny z panelem sterowniczym (a) i widok wnętrza (b)

## 2.1. EML functional modules

Each of five main RLC circuits consists of a capacitor bank (C) and a coil (L) connected in series. The equivalent resistance (R) in the circuit represents resistances of copper conductors and connectors. The function of current switching is realized by thyristors (on-state RMS current 1.6 kA, non repetitive surge peak on-state current 15 kA). Due to high instantaneous values of the current and heat losses, each thyristor is equipped with two radiators cooled with natural air flow (Fig. 2a).

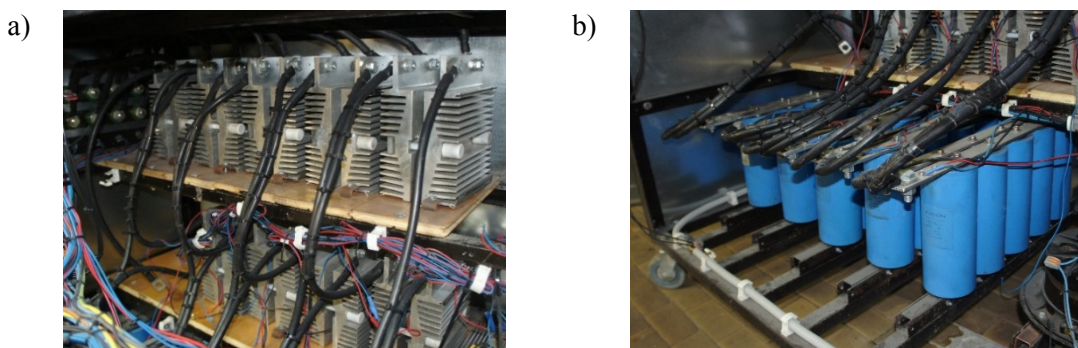


Fig. 2. Electromagnetic launcher – thyristors (a) and capacitor banks (b)  
Rys. 2. Wyrzutnia elektromagnetyczna – tyrystory (a) i banki kondensatorów (b)

In order to provide an optimal current-carrying capacity and high capacitance value, single capacitors ( $C = 15 \text{ mF}$ ,  $U_n = 350 \text{ V}$ ) are connected in parallel banks (Fig. 2b). The coils belong to the most important functional parts of the electromagnetic launcher. They are made with a copper conductor (cross-sectional area  $12.5 \text{ mm}^2$ , 100 turns, 2 layers, the internal coil diameter 10 mm, length 200 mm) and placed along the gun tube – see Fig. 3.

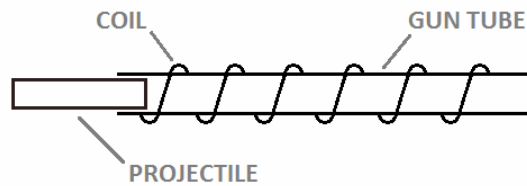


Fig. 3. EML coil and tube layout

Rys. 3. Położenie cewki na lufie wyrzutni elektromagnetycznej

The control module is based on ATMEGA328 microcontroller. Its main function consist in sending impulses responsible for triggering thyristors through their gate circuits. The moment of activation of electrical switches can be chosen by the user or set automatically by optical position sensors placed in the gun tube (Fig. 4).

The power supply module is based on the single-phase 230 V AC grid. The AC power is transformed to DC through an autotransformer followed by a bridge rectifier. The capacitor charging unit, which is detached for projectile launching cycle, provides charging current for capacitor banks. The measurement module (Fig. 1a) consists of ammeters and voltmeters monitoring parameters of the capacitors and power supply.



Fig. 4. Gun tube of the launcher with coil connectors visible

Rys. 4. Lufa wyrzutni z widocznymi zaciskami cewek

Remaining parts of the electromagnetic launcher include a case made from metal sheets and a welded metal frame. The coilgun is also equipped with wheels providing its mobility.

## 2.2. Projectile parameters

The coilgun is equipped with a gun tube which allows to accelerate cylinder-shaped steel projectiles with the diameter  $d = 8$  mm. All the experiments and simulations have been carried out for a projectile with the length  $l = 100$  mm and the mass  $m = 38$  g. Its relative permeability ( $\mu_r = 24.5$ ) have been measured (see Fig. 5) using the method described in [15], [17]. As the further experiments show, the projectile parameters influence the coilgun efficiency and should be chosen very carefully [5].



Fig. 5. Measurement setup for the projectile relative permeability measurements  
Rys. 5. Układ do pomiaru względnej przenikalności magnetycznej pocisku

### 2.3. Principle of operation

The coilgun under consideration contains five independent stages generating reluctance force which interacts with a steel projectile. The reluctance force is generated as a result of the magnetic field produced by coils in all stages. The main circuit can be reduced to a basic RLC circuit (Fig. 6) in which the resistance, inductance and capacitance are represented by lumped elements. Energy accumulated in the capacitor banks is released to the coil in a moment of thyristor triggering. Current flowing through the circuit is oscillating, but due to the presence of resistance it is highly damped.

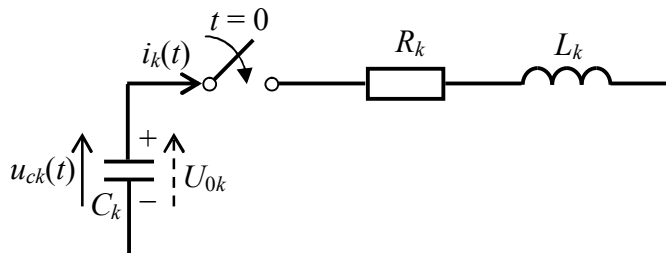


Fig. 6. Electrical diagram of the  $k$ -th main RLC circuit ( $k = 1, 2, 3, 4, 5$ )  
Rys. 6. Schemat obwodu głównego RLC numer  $k$  ( $k = 1, 2, 3, 4, 5$ )

Basic parameters describing the circuit (Fig. 6) include the lumped resistance  $R$ , the inductance  $L$  and the capacitance  $C$  as well as  $U_0$  – the voltage across the capacitors at the moment of switch closing (initial condition). This voltage also directly influences the current flowing in the main circuit. The waveform of this current, inter alia, has an impact on the value of the reluctance force interacting with the projectile.

Other very important factors influencing the reluctance force are construction of the projectile and its position in relation to the center of the accelerating coil. Depending on the intensity of the magnetic field generated by the coil, a linearized model of the magnetic circuit or a nonlinear one based on a nonlinear B-H curve can be applied. The model has an impact on the results, e.g. on the final acceleration of the projectile, especially in the case of saturation. The position of the projectile is also crucial in terms of effectiveness of the

acceleration process, because the reluctance force is always directed to the center of the coil. This means that the whole energy should be transferred before reaching the coil center by the projectile, otherwise a decrease of the velocity, and what follows the efficiency, is observed.

### 3. EML SIMULATION

In order to describe an impact which the phenomena described in the previous section have on the projectile and the efficiency of the electromagnetic launcher, a simulation model of the device has been proposed. It allows to simulate the whole duty cycle of the real device. The emphasis has been placed on providing a solution which does not require a commercial software. It has also been important to provide the highest simplicity of the solution while maintaining the required precision.

The main postulate of the analysis consists in braking up the whole continuous effects occurring in the electromagnetic launcher into minor components – uniformly accelerated motions. It allowed application of discrete analysis based on basic dynamic formulas, such as kinematic motion equation for the described kind of motion.

The master program (Fig. 7) has been designed in the Scilab environment [3]. The second very important element of the simulation is a FEMM based model [13], [14]. The field analysis conducted by the finite elements method allows to avoid the application of complicated mathematic formulas expressing the projectile acceleration as a function of the magnetic field. A special Scilab script enables controlling FEMM software through implemented Lua-script. This fact is crucial from the continuity of calculation point of view, because it allows building a loop which eliminates necessity of the user interference during the calculations. The same approach has been successfully applied in the case of power flow calculations [12].

The transient state occurring in the RLC circuit has been described numerically in the Scilab environment. The formulas used in the simulation are the result of analysis of a typical RLC circuit with an initial condition originating from the pre-charged capacitor.

Assumptions made in the project include omitting resistance to motion, that is sliding friction interfering with a projectile and air resistance connected with the pressure in the gun tube. Additional circuit assumptions have also been made. They refer to the idealization of the RLC circuit with lumped parameters. Moreover, the influence of the transient effects during a thyristor turning on has been omitted, although stationary active-state resistance has been taken into account. The project also assumes that the inductance of the coil is independent on the projectile displacement.

The input data for the proposed algorithm (Fig. 7) include system parameters as well as the initial condition, which are used for calculating the instantaneous value of the current and then for computing the reluctance force through the FEMM software. The next step refers to basic physics formulas used for calculating the displacement of a projectile during a given time interval. If the displacement differs from an assumed step size, a correction of the time interval takes place and the analysis is repeated. Otherwise, the velocity is calculated and the projectile position is changed. Next, all the calculations are repeated with new initial conditions – the non-zero displacement and the initial velocity being the end velocity from the previous step. The program operates until the projectile leaves the gun tube.

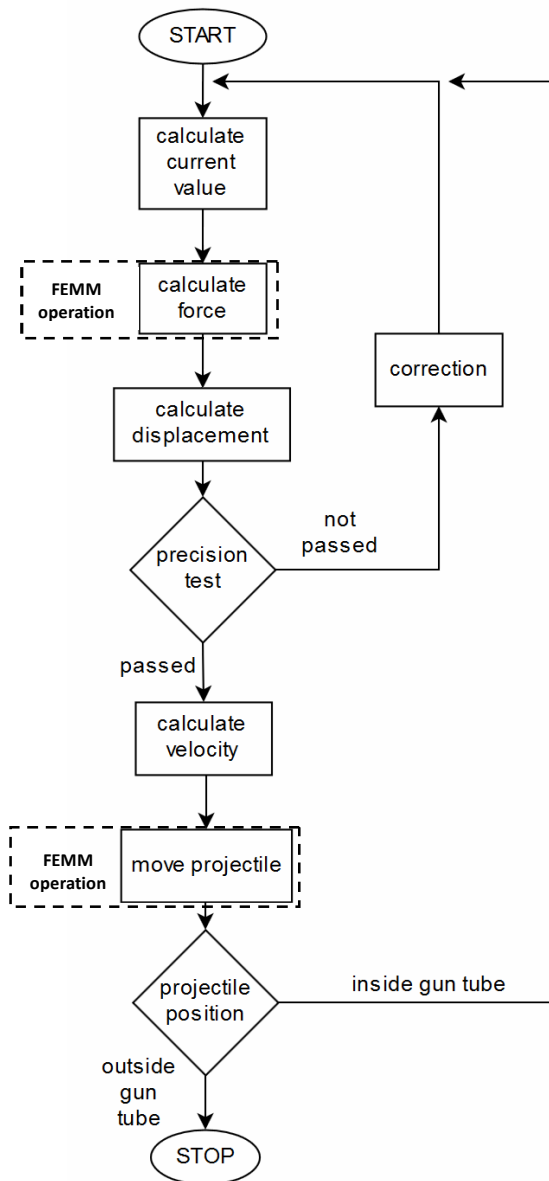


Fig. 7. Block diagram of the Scilab-implemented algorithm

Rys. 7. Schemat blokowy algorytmu zaimplementowanego w programie Scilab

#### 4. SELECTED SIMULATION RESULTS

As the initial efficiency measurements conducted for the real device consisted only of one stage tests, the simulations in this paper have also been limited to a single stage launcher. However, the algorithm and the models are ready for modelling the multistage launcher – see [4].

Computer simulations have been conducted for a few alternative scenarios so as to allow us to present the most important effects occurring during the projectile launch in the coilgun. This particular model has been oriented on the detailed analysis of the beginning phase of a shot, mainly it covers basic relations between the displacement, velocity and acceleration of

an object in the first coil for various initial conditions and other parameter values. Some results obtained for all five stages of the EML can be found in our earlier work [4].

Initially, the static analysis has been conducted in order to consider relation between the reluctance force and its location in or near an accelerating coil powered by a DC source (Fig. 8). The calculations have been repeated for different values of the magnetic permeability of the projectile material in the case of a linear B-H curve (Fig. 9b) as well as for a nonlinear B-H curve (Fig. 9a) – considering magnetic circuit saturation.

For a given and constant current, the force highly depends on the projectile position  $x$  (Fig. 9). The projectile inside the coil is attracted in the direction of its center regardless of the projectile position and its material. This is why the circuit should be switched off before the projectile reaches the coil center. Otherwise, the force will slow it down. The force waveform and its maximum value depend on the current value and magnetic properties of the projectile material, i.e. the value of permeability for linear models (Fig. 9b) and the B-H curve for nonlinear ones (Fig. 9a).

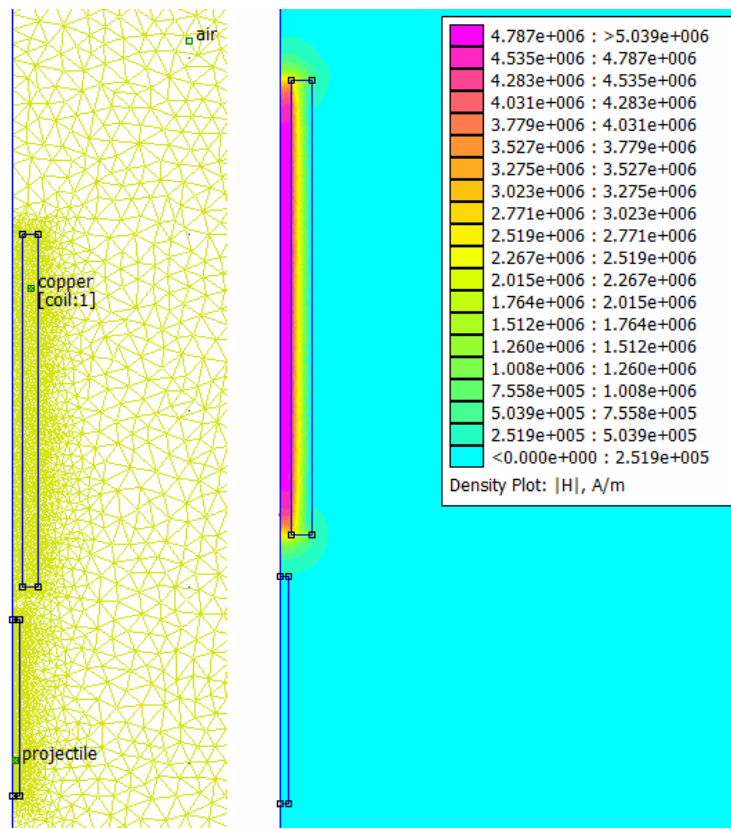


Fig. 8. FEMM model and exemplary simulation results  
Rys. 8. Model FEMM wraz z przykładowym wynikiem symulacji

On the other hand, the current depends on the RLC parameters and the initial conditions. The simulations have been performed for different values of the initial conditions and assuming constant values of the RLC parameters (measured for the real device). The current waveforms for the main RLC circuit (Fig. 6) have been shown in Fig. 10.

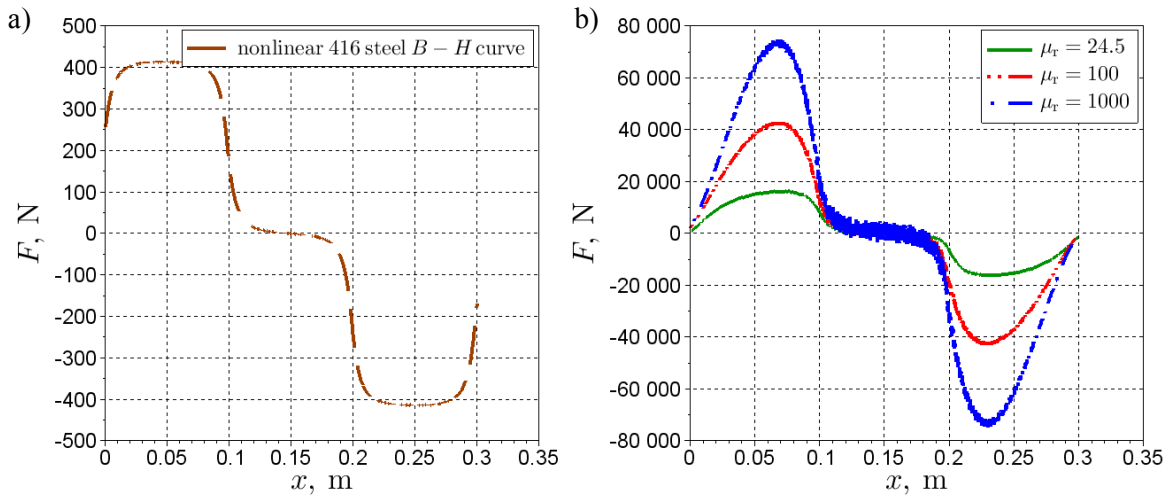


Fig. 9. Force-displacement plots for nonlinear (a) and linear (b) projectile materials ( $I = 10$  kA)  
Rys. 9. Wykresy siły w zależności od położenia pocisku dla nieliniowych (a) i liniowych (b) materiałów ( $I = 10$  kA)

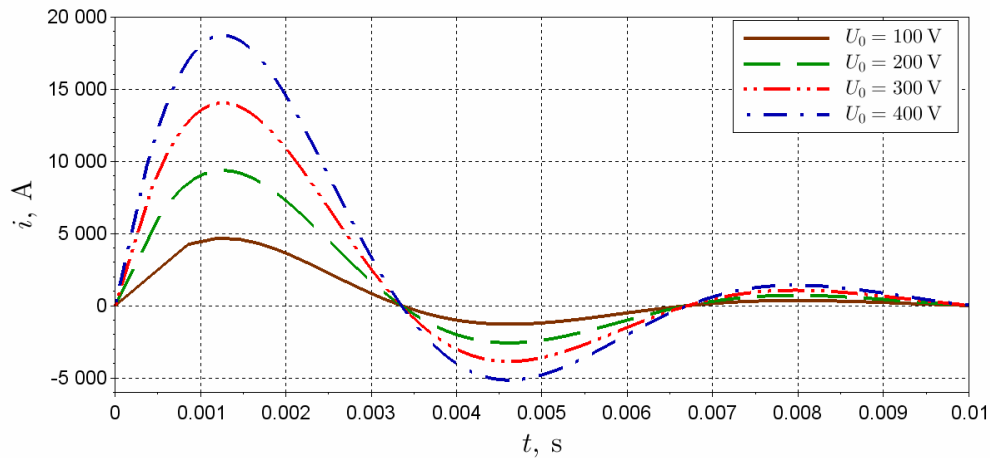
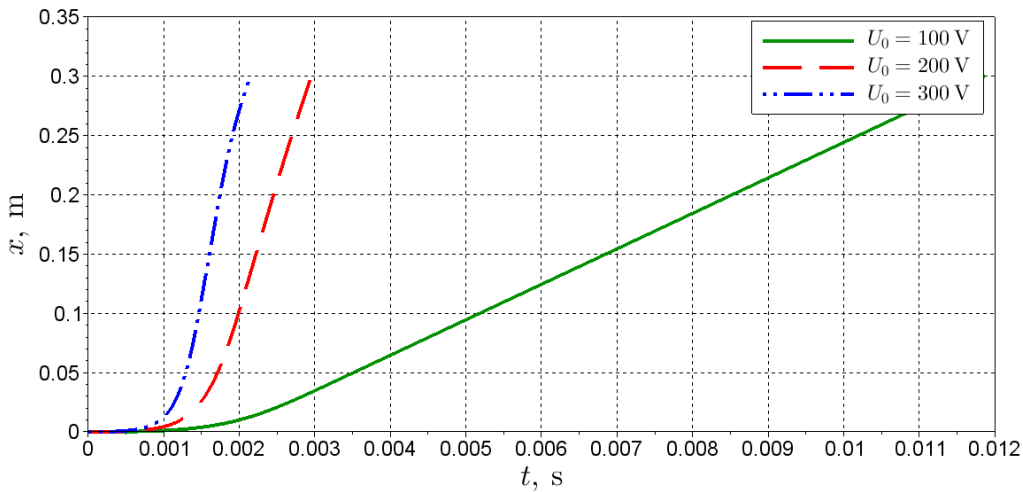
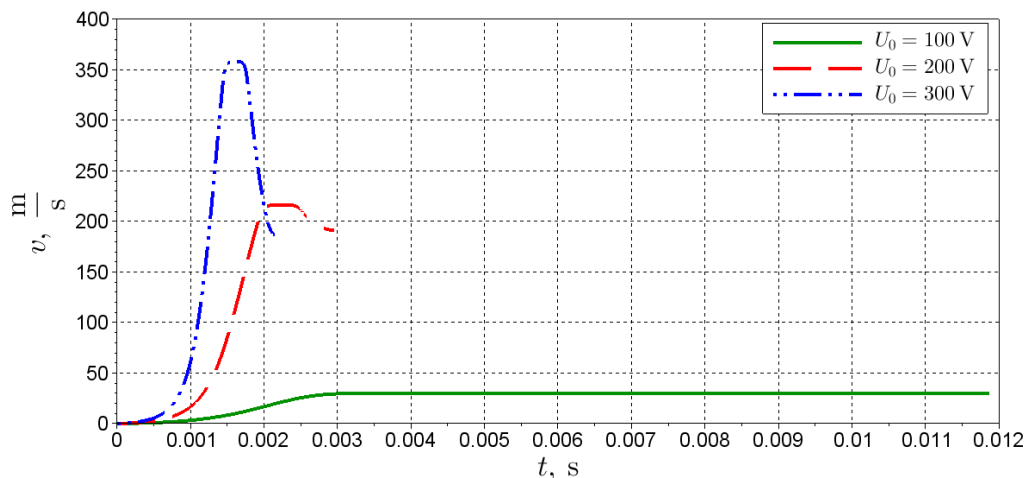
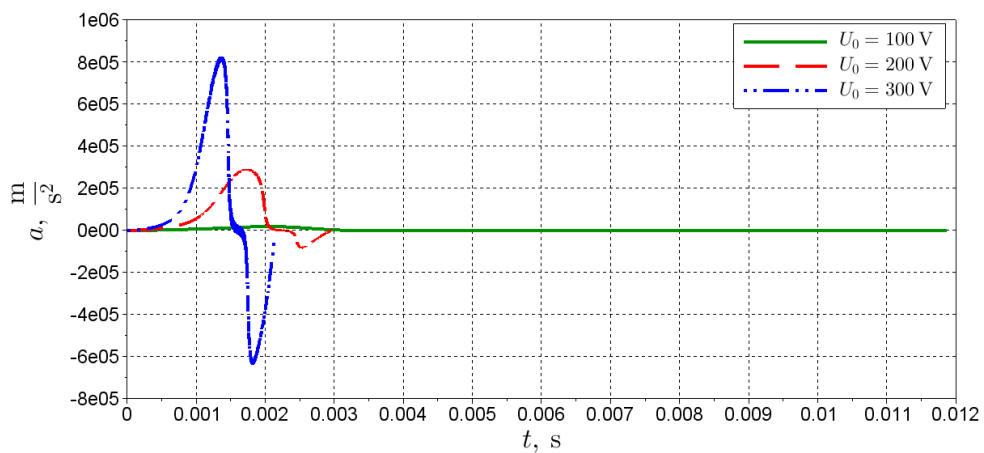
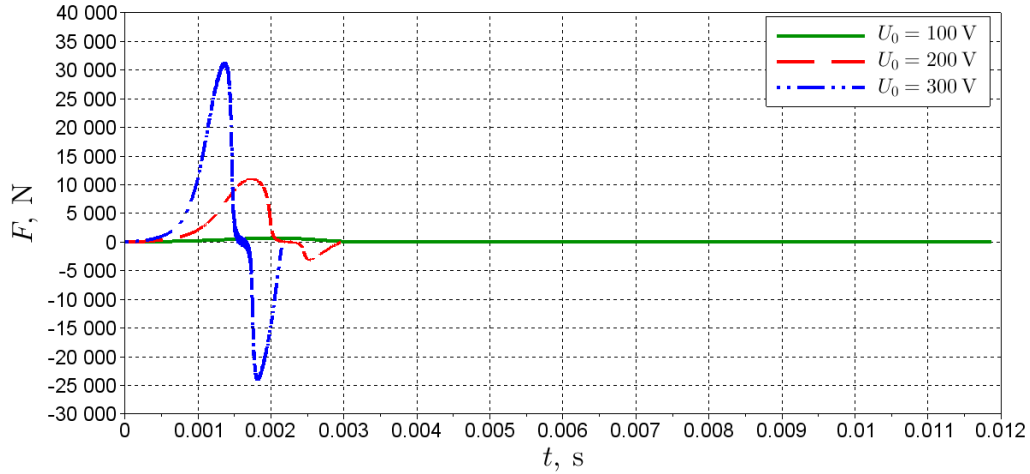


Fig. 10. Current time waveforms in the main RLC circuit for different  $U_0$  values  
Rys. 10. Przebiegi czasowe prądu w głównym obwodzie RLC dla różnych wartości napięcia  $U_0$

The waveforms presented in Fig. 10 have been obtained assuming that the RLC circuit remains switched on even if the current changes its polarity. It must be stressed that further simulations take into account that thyristors used as switching devices in the main RLC circuits switch off the circuit when it reaches zero, i.e.  $i(t) = 0$  for  $t > 0.0033$  s.

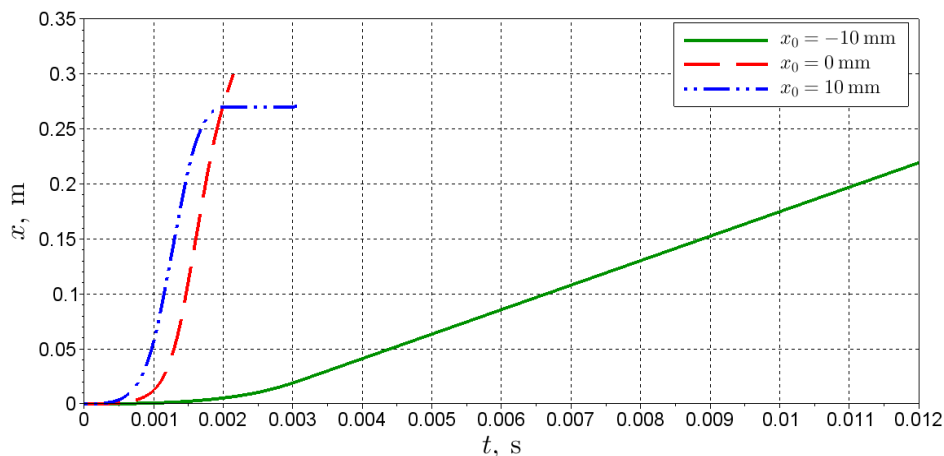
Combining the lumped RLC circuit analysis and the reluctance force calculation by FEM method resulted in a coherent dynamic model of the coilgun single stage. The model allowed us to determine waveforms of the displacement (Fig. 11), velocity (Fig. 12), acceleration (Fig. 13) and force (Fig. 14) for a real setup of the electromagnetic launcher with different initial conditions including the voltage across capacitor  $U_0$  as well as the starting position of the projectile  $x_0$ .

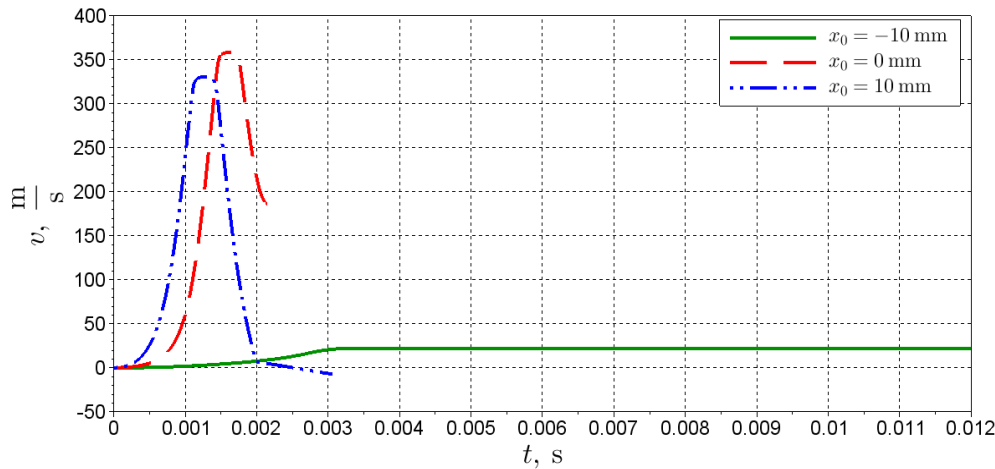
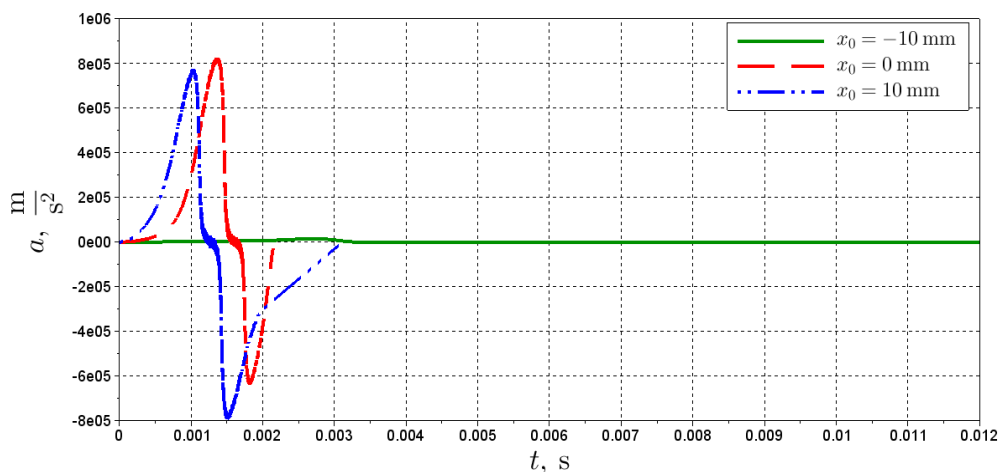
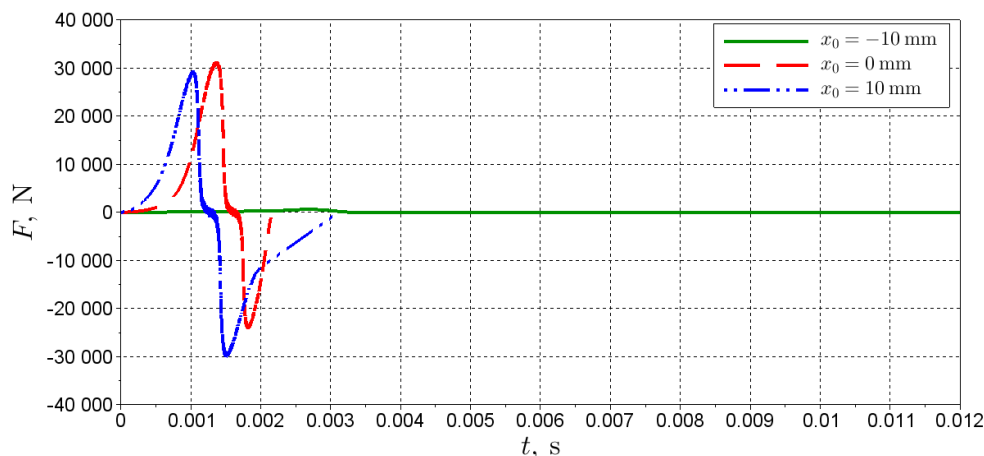
Fig. 11. Displacement plot for different  $U_0$  values ( $x_0 = 0 \text{ mm}$ )Rys. 11. Wykres przemieszczenia dla różnych wartości napięcia  $U_0$  ( $x_0 = 0 \text{ mm}$ )Fig. 12. Velocity plot for different  $U_0$  values ( $x_0 = 0 \text{ mm}$ )Rys. 12. Wykres prędkości dla różnych wartości napięcia  $U_0$  ( $x_0 = 0 \text{ mm}$ )Fig. 13. Acceleration plot for different  $U_0$  values ( $x_0 = 0 \text{ mm}$ )Rys. 13. Wykres przyspieszenia dla różnych wartości napięcia  $U_0$  ( $x_0 = 0 \text{ mm}$ )

Fig. 14. Force plot for different  $U_0$  values ( $x_0 = 0$  mm)Rys. 14. Wykres siły dla różnych wartości napięcia  $U_0$  ( $x_0 = 0$  mm)

The maximum value of the current waveform is proportional to the value of the initial voltage  $U_0$  (Fig. 10) and it directly influences the projectile behavior. The force, and so the acceleration, is proportional to the squared current and additionally it is influenced by the position of a projectile – compare Figs. 9, 10, 13 and 14. The current changes result in the corresponding changes of velocity (Fig. 12).

With the help of the described model, the initial location of a projectile  $x_0$  and its effect on the force and acceleration have also been considered (negative value of the initial location  $x_0$  corresponds to the front of projectile placed before the coil while positive one refers to the front of the projectile placed inside the coil).

Fig. 15. Displacement plot for different initial positions ( $U_0 = 300$  V)Rys. 15. Wykres przemieszczenia dla różnych położień początkowych pocisku ( $U_0 = 300$  V)

Fig. 16. Velocity plot for different initial positions ( $U_0 = 300 \text{ V}$ )Rys. 16. Wykres prędkości dla różnych położen początkowych pocisku ( $U_0 = 300 \text{ V}$ )Fig. 17. Acceleration plot for different initial positions ( $U_0 = 300 \text{ V}$ )Rys. 17. Wykres przyspieszenia dla różnych położen początkowych pocisku ( $U_0 = 300 \text{ V}$ )Fig. 18. Force plot for different initial position ( $U_0 = 300 \text{ V}$ )Rys. 18. Wykres siły dla różnych położen początkowych pocisku ( $U_0 = 300 \text{ V}$ )

The waveforms shown in Figs. 15-18 prove the relation between the force and the displacement reflected also in Fig. 9. The projectile placed initially further from the center of a coil is exposed to lower values of the force (Figs. 16 and 18,  $x_0 = -10$  mm) which results in lower kinetic energy values at the exit of the gun tube.

As shown in Figs. 14 and 18 in some cases a high value of the backward oriented force can occur and slow down the projectile. Two phenomena can be noticed:

- backward force caused by too fast acceleration resulting in the projectile passing the center of the coil sooner than the transient current dies out (Figs. 12 and 14,  $U_0 = 200$  V and 300 V),
- backward force caused by the initial position located too close to the center of the coil (Figs. 16 and 18,  $x_0 = 0$  mm and 10 mm).

An extreme case in which accelerated object is decelerated strongly enough to stop it before leaving a gun tube has also been simulated and presented in Figs. 15 and 16 ( $x_0 = 10$  mm).

The energy efficiency of the coilgun, defined as a ratio of the projectile kinetic energy to the capacitor stored energy, has been estimated for the analyzed above initial conditions and presented in Fig. 19. The efficiency value based on measurements is equal 0.6% for the initial voltage  $U_0 = 300$  V and  $x_0 = 0$  mm. The comparison of the measurement and the simulation result leads to a conclusion that the initial position of the projectile  $x_0$  during the measurements was not equal 0 mm. In the future the construction of the gun tube should be changed in order to enable to set the initial projectile position with high accuracy.

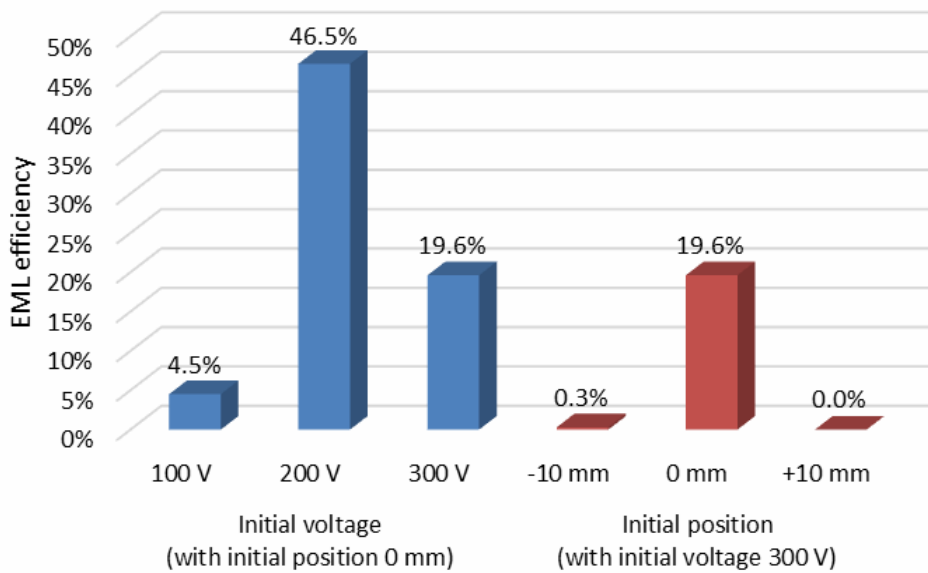


Fig. 19. EML efficiency bar graph

Rys. 19. Wykres słupkowy sprawności wyrzutni elektromagnetycznej

It must be stressed that relatively high values of the efficiency (Fig. 19) obtained just for a single stage are caused by simplifying assumptions in the simulated model, e.g. the lack of friction. Such assumptions are very often made in the research on EMLs [1], [8]. The assumptions change the quantitative results but the qualitative results remain correct.

The simulation results show the nonlinear and complex dependency between the coilgun efficiency and the initial conditions. In the future the best solution should be found by some optimization methods. The coilgun design belongs to complex problems and includes many decision variables described by complicated relations.

## 5. CONCLUSIONS

Despite of the fact that applying complicated mathematical calculus was not necessary in this particular project, a discrete modelling of multi-stage electromagnetic launchers requires comprehensive tools and computing power. Moreover, these requirements increase along with the number of stages and simplifying assumptions left. The risk of numerical errors and convergence problems is high and this fact results in necessity of applying rigorous precision requirements.

The obtained simulation results are consistent with theoretical expectations and moreover they have proved that the FEMM and Scilab software are efficient tools for multistage electromagnetic launcher simulations. Aspects in which simulation results can differ from real waveforms are related to simplifying assumptions, from which ignoring an impact of friction along with assuming the constant inductance are the most important. The changes of the inductance interfere with the current flow and as a result they cause deformation of the reluctance force. The air resistance factor has been considered during the simulations but its influence on the behavior of a projectile, comparing with the reluctance force, has been found to be almost unnoticeable and so it has been omitted.

Along with rising the initial voltage  $U_0$ , the velocity of the projectile also rises, but extending its value without optimizing launcher construction can result with an unwanted effect of the kinetic energy loss. The projectile slows down after passing the center area of a coil before transient current in the considered coil declines. In this case the RLC parameter change should be considered.

Many different factors have influence on the efficiency of the projectile acceleration. Mainly, the relation between the end of the transient state in the main circuit and the moment of passing the center of a coil by the projectile has to be analyzed. Finding an optimal case requires proper selection of the coil size as well as the initial position and the initial voltage.

The conducted simulations demonstrate that many aspects of the construction of the electromagnetic launcher under consideration can still be optimized.

## REFERENCES

1. Domin J.: Sprzęzony model polowo-obwodowy wyrzutni elektromagnetycznej. Rozprawa doktorska. Gliwice 2012.
2. Fair H.D.: Advances in electromagnetic launch science and technology and its applications. "IEEE Transactions on Magnetics" 2009, vol. 45, no. 1, pp. 225-230.
3. Gomez C. (Ed.): Engineering and scientific computing with Scilab. Springer Science & Business Media, New York 2012.

4. Grabowski D., Klimas M., Tylutki P.: Five-stage electromagnetic launcher computer simulations. XL Konferencja z Podstaw Elektrotechniki i Teorii Obwodów SPETO, 17-20.05.2017 Ustroń, pp. 27-28.
5. Holzgrafe J., Lintz N., Eyre N., Patterson J.: Effect of projectile design on coil gun performance. Franklin W. Olin College of Engineering, Needham 2012.
6. Hundertmark S.: Applying railgun technology to small satellite launch. 5<sup>th</sup> IEEE International Conference on Recent Advances in Space Technologies, 2011 Istanbul, pp. 747-751.
7. Jun H., Yuan P., Junija H.: Study of employing railguns in close-in weapon systems. "IEEE Transactions on Magnetics" 2009, vol. 45, no. 1, pp. 641-644.
8. Kaye R. J.: Operational requirements and issues for coilgun electromagnetic launchers. "IEEE Transactions on Magnetics" 2005, vol. 41, no. 1, pp. 194-199.
9. Kluszczyński K., Domin J.: Two module electromagnetic launcher with pneumatic assist. Modelling, computer simulations and laboratory investigations. "COMPEL: The International Journal for Computation and Mathematics in Electrical and Electronic Engineering" 2015, vol. 34, no. 3, pp. 691-709.
10. Krocze R., Domin J., Kluszczyński K.: Przegląd rozwiązań konstrukcyjnych wyrzutni elektromagnetycznych oraz ich klasyfikacja. II Kongres Elektryki Polskiej, 1-2.12. 2014 Warszawa, pp. 389-398.
11. Krocze R.: Metodologia projektowania, zagadnienia konstrukcyjne, modelowanie oraz badania wyrzutni elektromagnetycznej o napędzie hybrydowym. Rozprawa doktorska. Gliwice 2014.
12. Lewandowski M, Maciążek M., Grabowski D.: Integration of Matlab and PCFLO for harmonic flow analysis in a power system containing APF. XXXIV Międzynarodowa Konferencja z Podstaw Elektrotechniki i Teorii Obwodów IC-SPETO, 18-21.05.2011 Ustroń, pp. 89-90.
13. Meeker D.: Finite Element Method Magnetics. Dostępny w WWW: <http://www.femm.info/Archives/doc/manual42.pdf>. [Dostęp: 27.04.2017].
14. Meeker D.: Finite Element Method Magnetics: OctaveFEMM. Dostępny w WWW: <http://www.femm.info/Archives/doc/octavefemm.pdf>. [Dostęp: 27.04.2017].
15. Piaskowy A., Skórkowski A: Study of properties of paramagnetic and diamagnetic materials. XLV Międzyuczelniana Konferencja Metrologów MKM, 8-11.09.2013 Głucholaży, CD-ROM, pp. 1-4.
16. Seog-Whan K., Hyun-Kyo J., Song-Yop H.: Optimal design of multistage coilgun. "IEEE Transactions on Magnetics" 1996, vol. 32, no. 2, pp. 505-508.
17. Skubis T.: Metoda i układ do pomiarów przenikalności magnetycznej stali paramagnetycznych. IV Krajowe Sympozjum Pomiarów Magnetycznych, Kielce-Borków, 12-14.10.1994 Kielce, pp. 263-270.
18. Tao Z., Wei G., Fuchang L., Zizhou S., Honghai Z., Yanhui C., Mingtao L., Xiaochao S.: Design and testing of 15-stage synchronous induction coilgun. "IEEE Transactions on Plasma Science" 2013, vol. 41, no. 5, pp. 1089-1093.
19. Xi T., Shuhong W., Youpeng H., Song W., Yuqiong W.: Geometry and power optimization of coilgun based on adaptive genetic algorithms. "IEEE Transactions on Plasma Science" 2015, vol. 43, no. 5, pp. 1208-1214.

20. Zhang T., Guo W., Lin F., Cao B., Dong Z., Ren R., Huang K., Su Z.: Experimental results from a 4-stage synchronous induction coilgun. "IEEE Transactions on Plasma Science" 2013, vol. 41, no. 5, pp. 1084-1088.

Maciej KLIMAS

Silesian University of Technology

Faculty of Electrical Engineering, Institute of Electrical Engineering and Computer Science

ul. Akademicka 10

44-100, Gliwice

Student Electrical Engineering College name Professor Stanisław Fryzy

e-mail: macikli392@student.polsl.pl

Dr hab. inż. Dariusz GRABOWSKI

Silesian University of Technology

Faculty of Electrical Engineering, Institute of Electrical Engineering and Computer Science

ul. Akademicka 10

44-100 Gliwice

tel. (32) 237-10-08, e-mail: dariusz.grabowski@polsl.pl

Dr inż. Anna PIASKOWY

Silesian University of Technology

Faculty of Electrical Engineering, Institute of Measurement Science, Electronics and Control

ul. Akademicka 10

44-100 Gliwice

tel. (32) 237-29-91, e-mail: anna.piaskowy@polsl.pl